Extraction of Essential Region in Gastric Area for Diagnosing Gastric Cancer Using Double Contrast X-ray Images

Koji Abe [1]   **Hideaki Nakagawa** [1]   **Masahide Minami** [2]   **Haiyan Tian** [3]

[1] Interdisciplinary Graduate School of Science and Engineering
Kinki University
3-4-1 Kowakae, Higashi-Osaka, Osaka 577-8502, Japan
Email: koji@info.kindai.ac.jp, nakagawa0623nara@gmail.com

[2] Graduate School of Medicine
the University of Tokyo
7-3-1, Hongo, Bunkyo-ku, Tokyo 113-0033, Japan
Email: maminami@dream.com

[3] Ministry of Education
Chongqing University
Chongqing 400044, China

Abstract

In a mass screening for gastric cancer, diagnosticians currently read several hundred stomach X-ray pictures at a time. To lessen the number of reading the pictures or to inform lesions to diagnosticians, computer-aided diagnosis systems for the cancer have been proposed. However, in every system, the gastric area or its part for the diagnosis has been manually extracted in extracting characteristics of figure patterns in the area. To deign full automatic computer-aided diagnosis for the cancer, this paper proposes a method for extracting the essential region in the gastric area of double contrast X-ray images. In the proposed method, considering characteristics of density distributions around objects of the barium-pool, the spinal column, and edge of the gastric area, the essential region is fixed by recognizing the bottom of the barium-pool, the right side line of spinal column, and the edge from right side to bottom of gastric area. Experimental results for the proposed method by conducting an existing system of discriminating normal and abnormal cases using 43 images including 11 abnormal cases have shown that there is no significant difference between both of the results by the existing system which extracts the region manually and with the proposal.

Keywords: medical image processing, computer-aided diagnosis, X-ray image, gastric cancer.

1 Introduction

In mass screenings for gastric cancer, due to financial reasons, double contrast X-ray pictures are generally used on behalf of CT, MRI or photogastroscope. In the screenings, diagnosticians always need hard labor because they read several hundred X-ray pictures at a time. Besides, since accuracy of the reading is strongly depended on experience of diagnosticians, it is hard for inexperienced doctors to read them well. Especially, importance of accurate reading and its education have been increased in recent years from activity the Japanese Government exports the studio car which equips the camera for taking stomach X-ray pictures to Asian countries. For the reasons, computer-aided diagnosis (CAD) systems for gastric cancer in X-ray images have been required as a second opinion for diagnosticians (Kita 1996, Maeda et al. 1998, Hasegawa et al. 1991, 1992, Yoshinaga et al. 1999). In addition, a CAD system for discriminating normal stomachs to lessen the number of the readings has been reported (Abe et al. 2011). In every of the systems, characteristics of normal cases or lesions are extracted as features by analyzing figure patterns of the gastric area or a part of the area in double contrast X-ray images. However, although every system needs to extract gastric area or region of interests (ROI), all of them extract the areas manually. The reason why the systems avoid recognizing the areas would be because it is very difficult to extract only the areas from the stomach X-ray images, where shades of several 3D objects such as ribs, the spinal column, barium-pools overlap each other on 2D space.

For the sake of the essential pre-processing in CAD systems of gastric cancer using double contrast stomach X-ray images, this paper proposes a method for extracting the essential region for the diagnosis in the gastric area. When diagnosticians read the images, they check the pattern of fold shades appeared in the gastric area. Hence, the essential region should at least include the area where the shades are appeared and results of diagnosis by the CAD systems which equip the proposed pre-processing should be very similar to ones without it.

In this paper, after the essential region is defined, the proposed method for extracting the region is presented. Then, performance of the proposed method is examined by comparison between discrimination re-
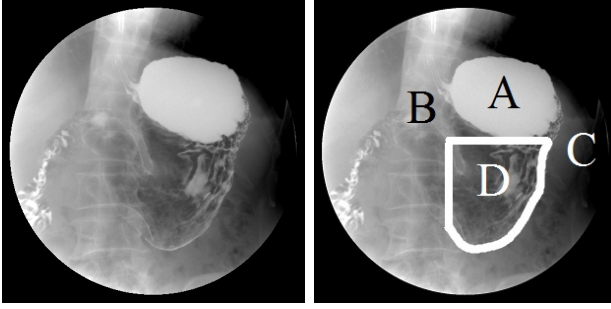
Figure 1: A double contrast stomach X-ray image and the essential region for the diagnosis (the area "D").

Figure 2: A result of the gastric area extracted by the snake algorithm.

sults of normal cases using the CAD system (Abe et al. 2011) and ones using the same system which equips the proposed method.

2 Double Contrast Stomach X-ray Images and the Essential Region for the Diagnosis of Gastric Cancer

In radiography to obtain contrast stomach X-ray pictures, participants drink barium and radiologists take eight X-ray pictures changing direction of their body. Diagnosticians first choose the head-on double contrast X-ray picture shown in Figure 1 among the eight pictures and diagnose the stomach reading it. When it is difficult to diagnose the stomach due to an uncertain or a doubtful case, the other pictures are used as the second material. Therefore, all the CAD systems of diagnosing stomach diagnose the head-on double contrast X-ray images. Hence, in this paper, the proposed method extracts the essential area for the diagnosis from the images as well.

The right image in Figure 1 is the copy of the left one, where "A" is the barium pool, "B" is the spinal column, "C" is the contour curve from the right side to the bottom of the gastric area, and "D" is the essential region. In the diagnosis, diagnosticians read the pattern of folds which mirror the shade of gastric rugae in the area D, which is located at the right side of B and under A in the images. Therefore, the essential region D is defined as the area which is enclosed by the right side line of B, the horizontal line through the bottom of the area A, and the curve C.

The active contour model (called as *Snakes*) (Kass et al. 1988) is often applied as a means for extracting the contour of an object (Fukushima et al. 2000). Figure 2 shows the contour of the gastric area extracted by applying the snake algorithm to one of the X-ray image, where the left shows a result of the contour recognition for the gastric area and the right shows the result of extracted gastric area. As shown in Figure 2 (right), the barium pool and a part of the spinal column have been included in the extracted area. Besides, some control points have invaded into the gastric area and the contour has chipped the right side part of the area. In radiography, since the human body, which is a 3D object, is mirrored into 2D space, 3D multi-organs are appeared to overlap each other in the 2D X-ray picture. Due to the overlaps, it is very hard for the snake algorithm to catch the
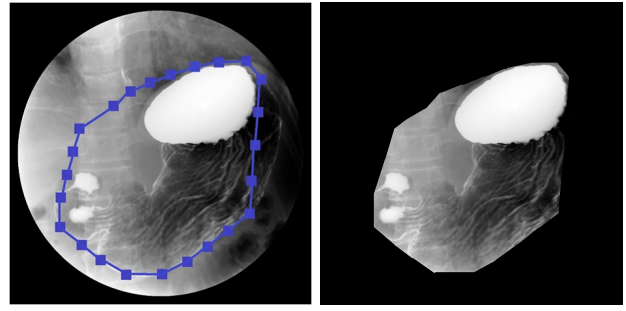
correct contour of gastric area in the X-ray images.

Thus, if the target area for the diagnosis lacks roughly or includes other objects, the CAD systems could not output correct results. Therefore, it is necessary to propose another way for extracting the essential region which does not include other organs and keeps the pattern of folds appeared in gastric area.

Throughout this paper, all the double contrast X-ray pictures are digitalized as images by CR (Computed Radiography). The size of the images is 1024 × 1024 pixels with 256 gray levels.

3 Proposed Method

3.1 Extraction of the barium pool

In order to obtain the head location of the essential region, the barium pool is extracted by the following processing. In the X-ray images, pixel values of the barium pool are certainly between 150 and 255, and the contour of barium pool appears remarkably. Considering these characteristics, first, all the pixels whose value is no more than 150 are converted into 0 (i.e., their color becomes the complete black.). Second, the smoothing processes by the moving average and the selective local averaging (Rosenfeld et al. 1982), edge enhancement by the Kirsh filtering (Parker 2010) are applied to the image in order. Third, the image is binarized into the black and white image by discriminant analysis and the thinning is applied to the image. Since the barium pool is basically located at the upper right in the image, the line segments obtained by the thinning whose part is not included in the quarter area at the upper right side in the image are removed. Figure 3(2) shows the image obtained by these processes from the original image of Figure 3(1).

Next, all the pixels in the quarter area at the upper right side of the original image are binarized by the threshold of pixel value 200. Figure 3(3) shows the cetroid point in the area extracted from Figure 3(1) and it is regarded as the central point of the barium pool. In radiating a straight line from the central point, the nearest intersection between the line and one of the line segments (shown in Figure 3(2)) is obtained as shown in Figure 3(4). The straight line radiates from the point at intervals of an angle of 7.5 degree, i.e., the number of the extracted intersections becomes 48 points. The contour of the barium pool
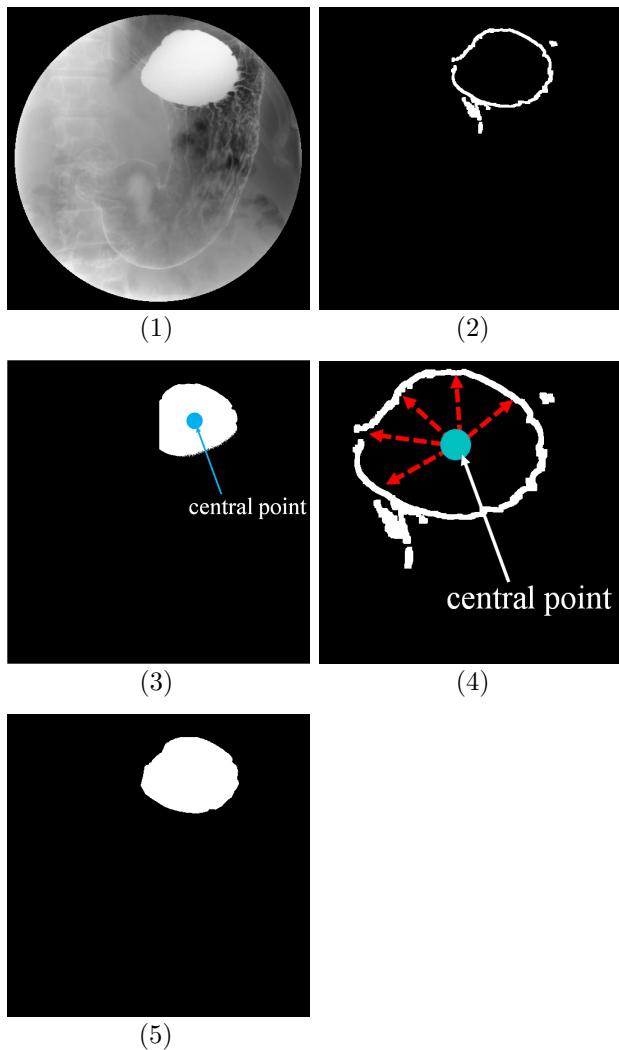
Figure 3: Processes for extracting the barium pool ((1)original image (2)line segments obtained as candidates of the contour of the barium pool (3)central point of the barium pool (4)the radiation of lines from the central point (5)extracted barium pool).
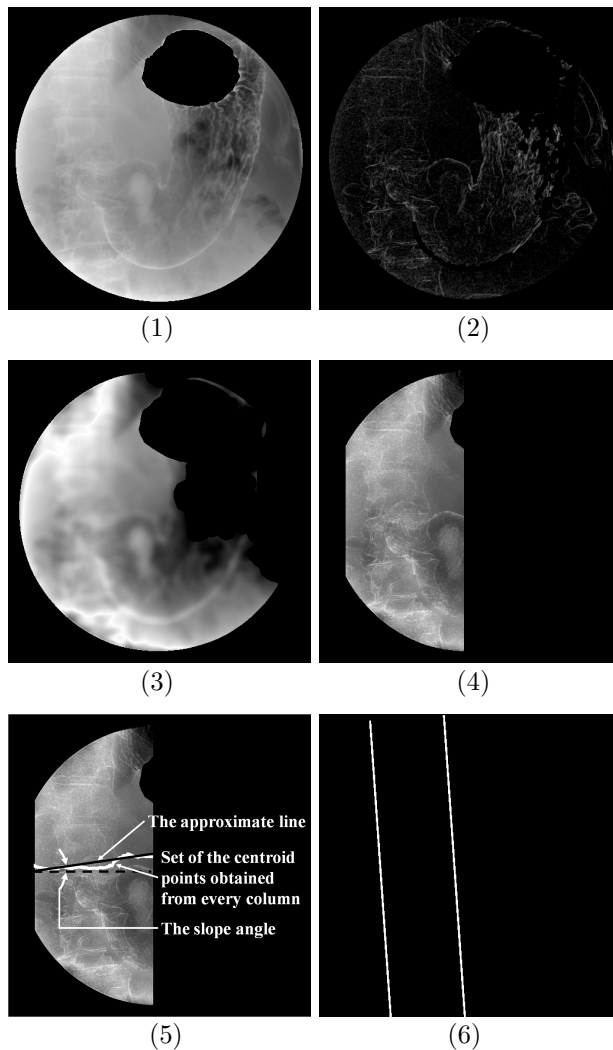

Figure 4: Processes for extracting the spinal column ((1)removal of the barium pool (2)image 1 (3)image 2 (4)candidate area for the spinal column (5)the slope angle of the spinal column (6)both sides of the spinal column).

is obtained by connecting neighbor intersections with the line segment between the intersections. Figure 3(5) shows area of the barium pool obtained from the contour.

3.2 Extraction of the spinal column

Before extracting the spinal column in the image, the area of barium pool is converted into black area in the image as shown in Figure 4(1).

Since difference of density between the spinal column and its background is not clear, Sobel filtering is applied to the image (Figure 4(1)) in order to enhance edge of the spinal column. Then, to reduce noises except the spinal column, pixels whose value is more then 50 and others which are located within a 3-pixels radius from them are removed. Figure 4(2) shows the result of this processing for Figure 4(1) and this image is called as *image 1* (Figure 4(2) is represented by threefold density of the actual one.). The frequency of folds' pattern appeared in the gastric area is higher than the spinal column. Hence, high-

frequency components are removed from the image shown in Figure 4(1) by the band-pass filter of 3 ∼ 255-radius after Fourier transformation and the pixel value of all the pixels is converted into twice after inverse Fourier transformation. Figure 4(3) is the result of this processing for Figure 4(1) and the image is called as *image 2*.

Next, two of the image 2 is superposed on and the image 1 besides the total value of all the pixel values on each column of the superposed image is calculated in every column. Since pixel values are hold down except the spinal column, the total value should be significantly high at columns in the spinal column. Besides, the width of the spinal column is around 250. Hence, the column which has the largest total value is found and columns which are horizontally more than 250 away from the column are removed. Figure 4(4) shows the result of this processing for Figure 4(1) and this area is regarded as *candidate area for the spinal column*. Using pixels whose value is more than 100 in each column of the candidate area for the spinal column, g_{min} is found for obtaining the minimum value

$f(g_{min})$ of $f(g)$ shown in Eq.(1) and g_{min} is found from every column of the candidate area as the y-coordinate of the centroid point in the column.

$$f(g) = |\sum_{y=0}^{1023} f_y \times (g - y)| \qquad (1)$$

where y is y-coordinate of a pixel whose value is more than 100 in a column, and f_y is its value. After that, an approximate line is obtained using the pixels obtained from each column. The angle between the approximate line and the horizontal line is regarded as the slope angle of the spinal column. Figure 4(5) shows the angle.

Finally, among all the columns in the candidate area, only higher rank half of them, which have larger total value of all the pixel values in the column, are chosen as the spinal column. Here, among the half, independent columns are removed because it would be impossible that an independent line forms the spinal column. The bundle of the chosen columns is rotated at the slope angle around the central point of the whole image. Figure 4(6) shows the two lines at both sides of the bundle obtained from Figure 4(1), and the area between them is regarded as the spinal column.

3.3 Extraction of the contour from the right to the bottom of the gastric area

Since the gastric contour in the X-ray images is not appeared clearly in most of cases, Sobel filtering is applied to the original image. And, since the left side area of the right side line of the spinal column extracted in 3.2 is not necessary for the diagnosis, the area is removed.

The shape of gastric area is always changing, hence the gastric contour is not uniform in the stomach. Although it would be difficult to catch characteristics of the shape, the contour has characteristics that the contour is clearer than shades of bowel and density of the contour is higher than its background in the X-ray images. Considering the characteristics, after the processes shown above are conducted to the image, the image is binarized according to the following three conditions:

[Conditions for the binarization of the contour]

1. the pixel whose value is more than 35 and difference of pixel value between the pixel and the first or second nearest right and left pixels from the pixel is more than 5

2. the pixel whose value is more than 35 and difference of pixel value between the pixel and the first or second nearest upper and lower pixels from the pixel is more than 5

3. the pixel whose value is more than 35 and difference of pixel value between the pixel and the nearest four pixels except pixels connected by the 4-neighbor connectivity among 8-neighborhoods of the pixel

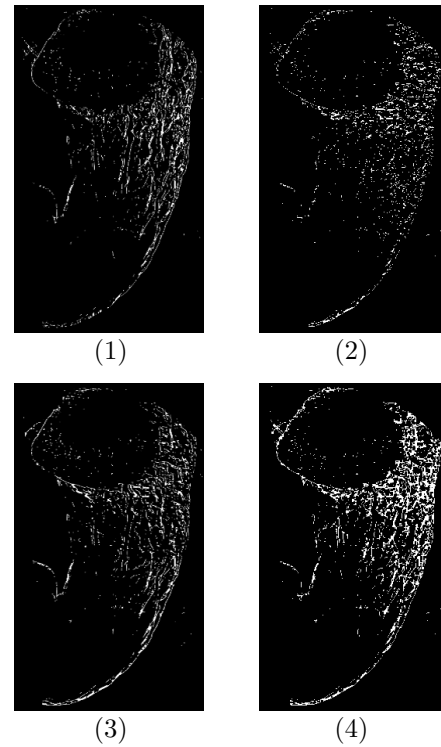This binarization produces one image to each condition (i.e., it produces three images.). After that,

Figure 5: The binarization according to the conditions ((4) is the final output in the binarization.).
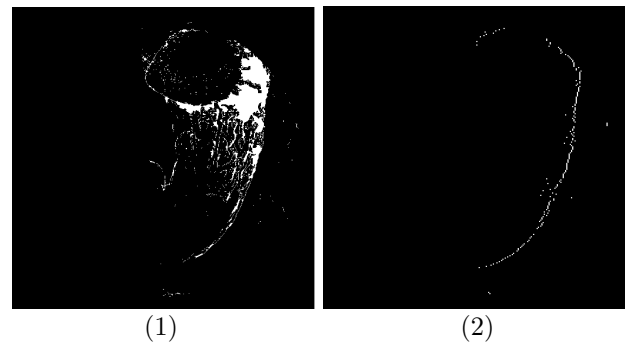

Figure 6: The process for obtaining the candidate points on the contour of the gastric area.

noises are removed by the combination of dilatation and erosion and the removal of isolated points in each of the three images, and the three images are converted into one image by OR composition. Figure 5 shows the results of the binarization to the image shown in Figure 3(1), where (1), (2), and (3) are the images binarized by the first, second and third conditions, respectively. And, Figure 5(4) shows the composite image of Figure 5(1), (2), and (3).

The contour curve from the right side to the bottom of the gastric area is extracted from the binary image obtained above as follows. First, all of closed black areas enclosed the white pixels are converted into the white color. Figure 6(1) shows the result of this processing for Figure 5(4). And then, dividing each of the vertical and horizontal sides into 256 in the image, a set of 4×4 pixels is regarded as 1 block, i.e., an image of 1024×1024 pixels is equal to 256×256 blocks. Second, scanning every block row
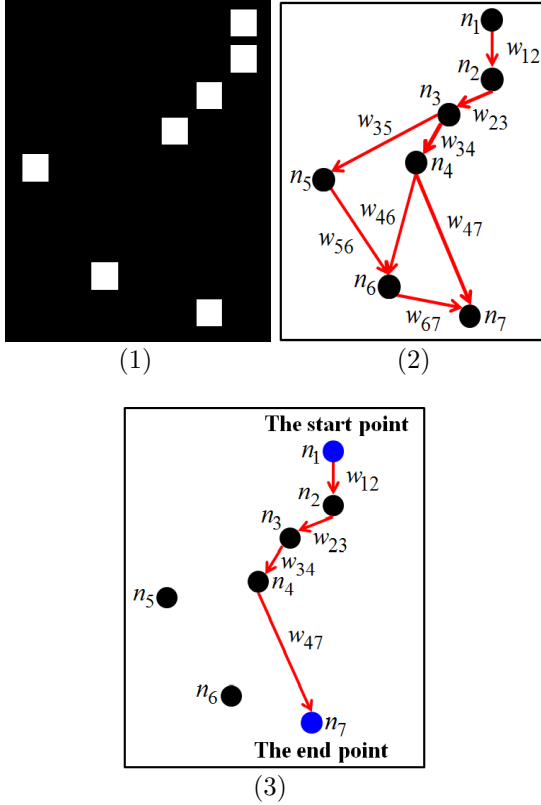
(1)   (2)

Figure 8: The candidate of the contour extracted from Figure 6(2).

(3)

Figure 7: The interpolation of the contour candidate by the DAG.

(1)   (2)

Figure 9: The tracking of the contour ((1)for the upper direction (2)for the lower direction).

horizontally in the image, the right end among the blocks which at least have 6 white pixels in every row is obtained. Among the obtained blocks, if upper end of the block is lower than the horizontal line which includes the bottom of the extracted barium pool, the upper right pixel in the block is extracted as a candidate point p on the contour. Figure 6(2) shows the set of the candidate points extracted from Figure 6(1). And, if a couple of the points (p_i and p_j) is satisfied with Eq.(2), the couple is connected by a line segment where the points become the line ends; and the line segment has a weight w_{ij}, which is the distance between the two points. Conducting it to every combination of the couples, directed acyclic graphs (DAGs) (Jungnickel 2013) are obtained to the image. In the DAGs, the points and the line segments are regarded as nodes and directed arcs, respectively, besides all the arcs are directed downward in the graph. Figure 7(1) shows a part of Figure 6(2) and Figure 7(2) shows a DAG obtained from Figure 7(1). Choosing only the DAG which has the number of the nodes most in all the DAGs, regarding the node which is at the highest location in the image as the start point and the node which is at the lowest location as the end point, the shortest route from the start point to the end point is obtained (Jungnickel 2013) as shown in Figure 7(3), and the track of the route is regarded as the candidate of the contour. Figure 8 shows the extracted candidate of the contour from Figure 6(2), where the left is the candidate and the right is the image which places the left on its original image.

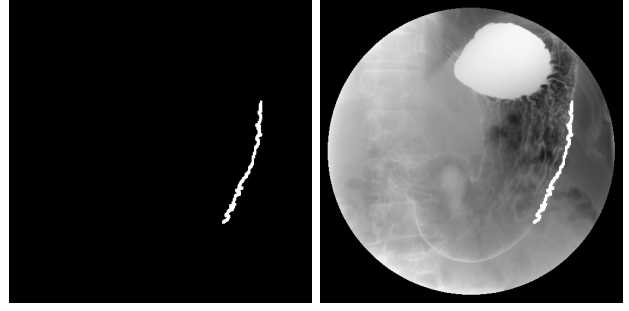$$|d_x(i,j)| \leq 5 \quad \wedge \quad S(i,j) \leq 30 \qquad (2)$$

where $d_x(i,j)$ and $S(i,j)$ are difference of x-coordinates and distance between p_i and p_j, respectively, i.e., $S(i,j)$ is $w(i,j)$ when a couple of p_i and p_j is satisfied with Eq.(2).

Next, individual white areas which are no more than 15 pixels are removed from the image that all of closed black areas enclosed the white pixels are converted into the white color obtained above (Figure 6(1)). The obtained image is called as *reference image*. Referring to the reference image, the contour is finally obtained by connecting n control points according to the tracking way shown below. Here, $I_u[i]$ and $I_l[i]$ are the i-th control point from the upper end $I_u[0]$ and the lower end $I_l[0]$ in the candidate of the contour, respectively. And then, n_u and n_l are the number of the control points obtained from $I_u[0]$ and $I_l[0]$, respectively (i.e., $n = n_u + n_l$).

[Flow of the interpolation]

1. The white pixels which are located at upper area from $I_u[i]$ (or, at lower area from $I_l[i]$) and satisfied with Eq.(2) in partnering $I_u[i]$ (or, $I_l[i]$) are searched in the reference image. Among them, the nearest pixel from $I_u[i]$ is set as $I_u[i+1]$ ($I_l[i+1]$ is set to the nearest pixel vertically and the farthest pixel horizontally from $I_l[i]$). If the suitable pixel is nothing, go to 3.

2. The white pixels which have y-coordinate of $I_u[i+1]$ (or, $I_l[i+1]$) and are satisfied with Eq.(2) in partnering $I_u[i+1]$ (or, $I_l[i+1]$) are searched in the reference image. $I_u[i+1]$ is moved to the pixel which has the largest x-coordinate. $I_l[i+1]$ is moved to the pixel which has the smallest x-coordinate. If nothing, go back to 1. increasing 1 to i.
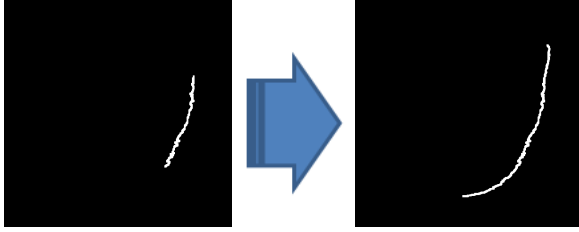
Figure 10: Extraction of the contour from the right side to the bottom of the gastric area (left: the candidate of the contour (Figure 8), right: the final output of the contour).
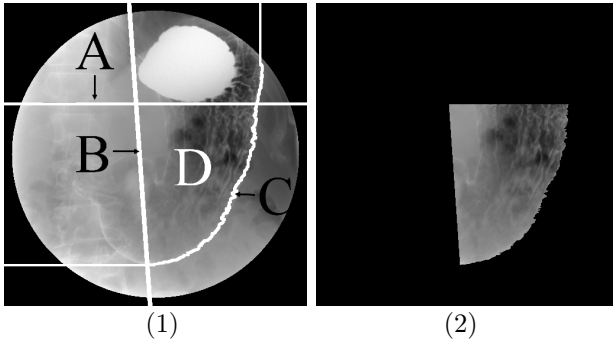

Figure 11: Extraction of the essential region ((1)composition of the extracted objects (2)the extracted essential region).

Table 1: Experimental results of the extractions for the three objects.

	success	failure
barium pool	42 cases (97.67%)	1 case
spinal column	42 cases (97.67%)	1 case
the outline	41 cases (95.35%)	2 cases
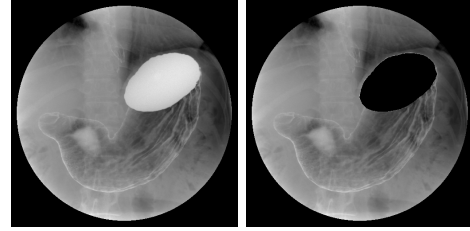
(1) a success case
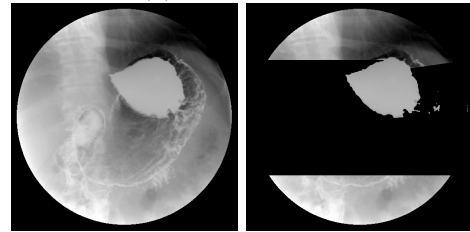
(2) the only failure case

Figure 12: Sample of results in the extraction of the barium pool.

3. Connect between $I_u[i]$ and $I_u[i+1]$ (or, $I_l[i]$ and $I_l[i+1]$) with a line. And, repeat it from $i = 0$ to $i = n_u$ (to $i = n_l$ in the case of $I_l[i]$).

As an example of the tracking, Figure 9 shows the tracking, where (1) shows the tracking from $I_u[0]$ to $I_u[3]$ and (2) shows from $I_l[0]$ to $I_l[3]$. Resulting this tracking, the contour is obtained finally. Figure 10 (right) shows the result of the contour obtained from the contour candidate for Figure 4(1).

3.4 Extraction of the Essential Region for the Diagnosis

The vertical line is drawn upward from the upper end of the contour extracted in 3.3. And, the horizontal line is drawn leftward from the lower end. The essential region is obtained by enclosing the horizontal line which includes the bottom point of the extracted barium pool obtained in 3.1 (A in Figure 11(1)), the right side line of the spinal column obtained in 3.2 (B in Figure 11(1)), and the curve which is the contour obtained in 3.3 plus the lines drawn here (C in Figure 11(1)). D in Figure 11(1) shows the essential region for the diagnosis. And, Figure 11(2) shows the final output of the essential region.

4 Experimental Results

### 4.1 The Extraction of the Essential Region

The proposed extractions for the three objects of 1)barium pool, 2)spinal column, and 3)the contour from the right side to the bottom of gastric area are applied in turn to 43 double contrast X-ray stomach images (32 normal cases, and 11 abnormal cases: all the abnormal cases had been diagnosed as gastric cancer by a medical doctor.). Performance of the extractions is evaluated by a medical examiner's eyes. After that, the essential region is extracted to only the images which got the extraction success in all the extractions of the three objects.

Table 1 shows experimental results of the extractions for the three objects. From the fact that the success ratios show more than 95 % in all the extractions, experimental results shown in Table 1 show that the proposed method has high performance in each of the extractions.

In the extraction of barium pool, according to the criterion of extraction success that at least 90 % of the pixels in the extracted area by the proposed method is included in the correct barium pool obtained by hands, only a case was failure. All the correct barium pools have been obtained by a nondoctor. Figure 12 (1) and (2) show a case of the extraction success and failure, respectively. The reason of the failure is because the central point was out of the correct area of barium pool. In this case, density of the barium pool was lower than the other X-ray images because some of barium ran into the intestine and barium decreased in the gastric area. Receiving this failure, it would be necessary to determine the threshold of the binarization considering the mean of density in the barium pool.

In the extraction of the spinal column, according to the criterion of extraction success that the extracted area includes at least part of the spinal column, only a case was failure and this failure case was
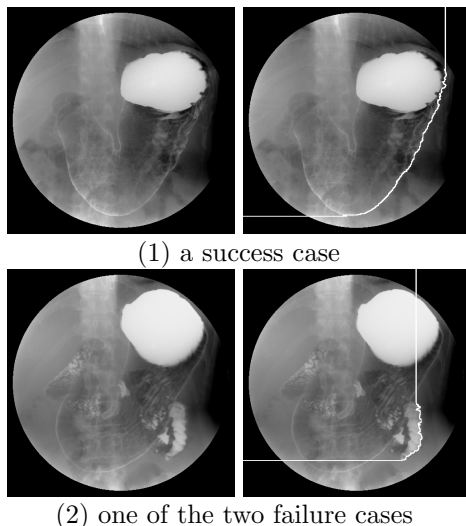
(1) a success case

(2) one of the two failure cases

Figure 13: Sample of results in the contour extraction.

(1)　　　　　　　　(2)

Figure 14: A case when the extracted contour was shorter than desirable length ((1)original image (2)result of the contour extraction).

the same as the case which was the failure in the extraction of barium pool. The reason of the failure is because the barium pool was not extracted precisely. Thus, the extraction of the spinal column is depended on the location of the barium pool.

In the extraction of the contour, according to the criteria of extraction success that the extracted contour is put on the correct contour and extraction failure that the extracted contour is completely out of the actual contour or the fold pattern is remarkably lacked due to too short contour, two cases were failure. Figure 13 (1) and (2) show a case of the extraction success and failure, respectively. In Figure 13(1), we can confirm the extracted contour is completely put on the actual contour from the right side to the bottom of the gastric area. On the other hand, in Figure 13(2), we can confirm the tracking error has been occurred. The reason for the failure case is because a mass of barium appeared on the contour located at the lower right has been tracked on behalf of the correct contour. And, since the extraction of the contour is depended on the locations of the barium pool and the spinal column, the image shown in Figure 12(2) got the failure in the contour extraction as well.

In 16 cases among the 41 cases which got success in all the extractions, the contour was a little shorter than desirable length. Figure 14 shows a case of them. However, since every of their essential regions includes fold patterns for the diagnosis enough, they were regarded as the extraction success. The reason why their contour has been shorter is because the noise removal in making the reference image has removed part of indispensable area to track the contour. Therefore, it is necessary to improve enhance the extraction of the candidate points on the contour.

4.2　The Discrimination of Normal and Abnormal Cases for the Essential Regions

By using the CAD system of discriminating gastric cancer (Abe et al. 2011), performance of the essential regions extracted by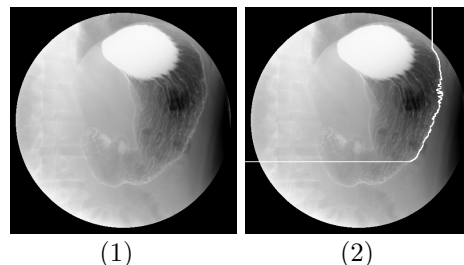 the proposal are compared with essential regions extracted by hands (used in Ref.(Abe et al. 2011)). All the essential regions extracted by hands have been obtained by a nondoctor. In the CAD system, image features proposed in Ref.(Abe et al. 2011) are extracted from the essential region and the discrimination is conducted by discrimination machines regarding the features as variables. As discrimination machines, linear discriminant analysis (LDA) the discriminant analysis by Mahalanobis' distance (MD), linear support vector machines (SVM) are applied for the discrimination. Before the image features for the diagnosis are extracted, the system extracts the folds in the essential region. The folds and the features are extracted as follows (Refer to (Abe et al. 2011) if necessary.).

The essential region is empirically binarized as follows. First, differences between every pixel value and each value of its 5 neighbors to each of right and left sides are measured, respectively. If the minimum difference among them is more than 16, the pixel is regarded as a pixel on a fold and its value is converted into 255. Otherwise, the value is into 0. Second, the binarization is conducted to every pixel in the vertical direction as well changing "5 neighbors" into "3 neighbors", and "right and left" into "upper and lower sides". Third, if the pixel value is 255 in one of the binarization images at least, the pixel value is fixed as 255. Otherwise, the value is 0. Finally, by conducting the thinning, the folds are extracted at last.

The features of parallelism f_1 and f_2 are extracted from the binary image of the folds as follows.

1) f_1 is defined as the number of pixels which have connection to at least three neighbors in 8-neighbor.

2) Removing all the points extracted in 1) from the binary image of the folds, all the folds are decomposed into line and curve segments. And then, one of the 8-direction codes is attached to every pixel on the folds in the image. The direction code d $(1 \leq d \leq 8)$ is assigned to the angle of $(d-1) \times \pi/4$ rotating counterclockwise from the horizontal direction from left to right. f_2 is defined as $f_2 = sum(max_1 + max_2)$, where max_1 is the number of pixels which have the most code in the image, max_2 is the number of pixels which have the second most code, and sum is the number of pixels which have the other codes.

Performance of the discrimination is represented

Table 2: Experimental results of the diagnosis for the essential region.

tool	normal		abnormal	
	Recall	*Pecision*	*Recall*	*Precision*
LDA	90.32% (28/31)	93.33% (28/30)	80.00% (8/10)	72.73% (8/11)
MD	67.74% (21/31)	91.30% (21/23)	80.00% (8/10)	44.44% (8/18)
SVM	87.10% (27/31)	93.10% (27/29)	80.00% (8/10)	66.67% (8/12)

Table 3: Experimental results of the diagnosis for the area extracted by hand.

tool	normal		abnormal	
	Recall	*Pecision*	*Recall*	*Precision*
LDA	90.32% (28/31)	93.33% (28/30)	80.00% (8/10)	72.73% (8/11)
MD	80.65% (25/31)	92.59% (25/27)	80.00% (8/10)	57.14% (8/14)
SVM	87.10% (27/31)	93.10% (27/29)	80.00% (8/10)	66.67% (8/12)

by ratios of *Recall* and *Precision* defined as

$$Precision = \frac{|X_h \cap X_c|}{|X_c|} \times 100 \qquad (3)$$

$$Recall = \frac{|X_h \cap X_c|}{|X_h|} \times 100 \qquad (4)$$

where X_h is the set of the correct answers, X_c is a set of images discriminated by the proposed method, and $|X|$ is the number of images of a set X.

In these experiments, the 41 images (normal case: 31, abnormal case: 10) which were extraction success in all the three extractions have been used. Table 2 and Table 3 show discrimination results for the essential regions by the proposal and by hands, respectively, where the numbers in parentheses are the number of images used to calculate the ratios. Both of the tables show that there is no significant difference between results of the discrimination using essential regions extracted by the proposal and by hands. Therefore, we could confirm that the extraction of the essential region by the proposed method would be efficient enough in the diagnosis for mass screening of gastric cancer.

5 Conclusions

To design a computer-aided diagnosis for gastric cancer, this paper has presented a method for extracting the essential region in the gastric area of double contrast X-ray images. In the proposed method, the barium pool, the spinal column, and the contour from the right side to the bottom of the gastric area have been extracted. The essential region is fixed by connecting the two lines extracted from the barium pool and the spinal column and by the contour curve of the gastric area. Experimental results for the proposed method by the existing system of discriminating normal and

abnormal cases have shown that there is no significant difference between both of the results by the existing system which extracts the region manually and by the proposal.

In the case when the angular incisur is included in the essential area, there is possibility that it becomes a noise and the CAD system leads to a discrimination error. As future works, it could be considered to improve the extractions of the central point in barium pools and the candidate points used to track the contour of the gastric area in addition to tracking the contour of the angular incisurs.

References

Y. Kita (1996), 'Elastic-model Driven Analysis of Several Views of a Deformable Cylindrical Object', *IEEE Trans. PAMI*, **18**(12), 1150–1162.

Y. Mekada, J. Hasegawa, J. Toriwaki, S. Nawano, and K. Miyagawa (1998), 'Automated Extraction of Cancer Lesions from Double Contrast X-ray Images of Stomach', *Proc. 1st International Workshop on Computer Aided Diagnosis*, Chicago, USA, 407–412.

J. Hasegawa, T. Tsutsui, and J. Toriwaki (1991), 'Automated Extraction of Cancer Lesions with Convergent Fold Patterns in Double Contrast X-ray Images of the Stomach', *Systems and Computers in Japan*, **22**(7), 51–62.

J. Hasegawa and J. Toriwaki (1992), 'A New Filter for Feature Extraction of Line Pattern Texture with Application to Cancer Detection', *Proc. 11th IAPR Int. Conf. on Pattern Recognition*, Hague, Netherlands, 352–355.

Y.Yoshinaga, H.Kobatake, and S. Fukushima (1999), 'The Detection and Feature Extraction Method of Curvilinear Convex Regions with Weak Contrast Using a Gradient Distribution Method', *Proc. ICIP 99*, Kobe, Japan, 715–719.

K. Abe, T. Nobuoka, and M. Minami (2011), 'Computer-Aided Diagnosis of Mass Screenings for Gastric Cancer Using Double Contrast X-ray Images', *Proc. IEEE Pacific Rim Conf on Communications, Computers and Signal Processing*, Victoria, Canada, 708–713.

M. Kass, A. Witkin, and D. Terzopoulos (1988), 'Snakes: Active contour models', *International J. of Computer Vision*, **1**(3), 321–331.

S. Fukushima, H. Uwai, and K. Yoshimoto (2000), 'Optimization-Based Recognition the Gastric Region from a Double-Contrast Radiogram', *IEICE Trans. (Japanese Edit.)*, **J83-D-II**(1), 154–164.

J.R.Parker (2010), 'Algorithms for Image Processing and Computer Vision', *Wiley Publishing*, 36–38.

A.Rosenfeld and A.C.Kak (1982), 'Digital Picture Processing, Second Edition, Volume 1', *Academic Press*.

D.Jungnickel (2013), 'Graphs, Networks and Algorithms', *Springer*, 49–52.